

# MEMS tunable VCSEL light source for ultrahigh speed 60kHz - 1MHz axial scan rate and long range centimeter class OCT imaging

Benjamin Potsaid<sup>1,2</sup>, Vijaysekhar Jayaraman<sup>3</sup>, James G. Fujimoto<sup>2</sup>,  
James Jiang<sup>1</sup>, Peter J.S. Heim<sup>4</sup>, Alex E. Cable<sup>1</sup>

<sup>1</sup>Advanced Imaging Group, Thorlabs, Inc., Newton, NJ 07860

<sup>2</sup>Department of Electrical Engineering and Computer Science and Research Laboratory of  
Electronics, Massachusetts Institute of Technology, Cambridge, MA 02139

<sup>3</sup>Praevium Research Inc., Santa Barbara, CA 93111

<sup>4</sup>Thorlabs Quantum Electronics Inc., Jessup, MD 20794

## ABSTRACT

This paper demonstrates new wavelength swept light source technology, MEMS tunable VCSELs, for OCT imaging. The VCSEL achieves a combination of ultrahigh sweep speeds, wide spectral tuning range, flexibility in sweep trajectory, and extremely long coherence length, which cannot be simultaneously achieved with other technologies. A second generation prototype VCSEL is optically pumped at 980nm and a low mass electrostatically tunable mirror enables high speed wavelength tuning centered at ~1310nm with ~110nm of tunable bandwidth. Record coherence length >100mm enables extremely long imaging range. By changing the drive waveform, a single 1310nm VCSEL was driven to sweep at speeds from 100kHz to 1.2MHz axial scan rate with unidirectional and bidirectional high duty cycle sweeps. We demonstrate long range and high resolution 1310nm OCT imaging of the human anterior eye at 100kHz axial scan rate and imaging of biological samples at speeds of 60kHz – 1MHz. A first generation 1050nm device is shown to sweep over 100mm. The results of this study suggest that MEMS based VCSEL swept light source technology has unique performance characteristics and will be a critical technology for future ultrahigh speed and long depth range OCT imaging.

**Keywords:** Optical Coherence Tomography, VCSEL, Swept Source, Medical Imaging, Ophthalmology

## 1. INTRODUCTION

First demonstrated in 1991<sup>1</sup>, OCT enables micron scale non-invasive 2D and 3D imaging of tissue and has become a clinical standard for the diagnosis and management of ocular disease<sup>2-5</sup>. According to Medicare reimbursement codes and statistics from eye centers, an estimated 16 million ophthalmic OCT procedures were performed in the US in 2010<sup>6</sup>. The most common commercial OCT system sold today is a retinal imaging instrument using spectral / Fourier domain detection at 850nm wavelengths and operating at speeds of ~20,000 to ~50,000 axial scans per second. Retinal imaging instruments can be converted for anterior segment imaging by using an external adapter lens<sup>7</sup>, however imaging range is limited to only ~2mm because of spectrometer resolution limits in the underlying spectral OCT technology. Dedicated imaging instruments use 1310nm wavelengths and time domain detection to achieve longer imaging ranges of ~6mm required for anterior segment imaging at 2kHz with 18um axial resolution (Zeiss Visante), or swept source OCT at 30kHz with 10um axial resolution (Tomey SS-1000). OCT is also used for intravascular imaging and research applications, however ophthalmic OCT imaging is the most mature field. Limitations and design tradeoffs in imaging range, imaging speed, and axial resolution when using existing OCT detection and source technologies has generally required compromise in instrument design and performance.

A new MEMS tunable VCSEL light source technology achieves a combination of ultrahigh sweep speeds, wide spectral tuning range, adjustability in sweep trajectory and extremely long coherence length, which cannot be simultaneously achieved with any other previously demonstrated OCT light source technology. The unique capabilities of the light source promise to improve existing OCT applications and enable new long imaging range centimeter class OCT applications. In this paper, we demonstrate the VCSEL for in vivo OCT imaging of the human eye for the first time.

We demonstrate record coherence lengths of much greater than 100mm with the VCSEL, which enables extremely long OCT imaging without compromising imaging speed or sweep range. We show that the sweep speed and sweep trajectory of the VCSEL can be changed simply by changing the electrical drive waveform. This paper first reviews OCT imaging technology in Section 2. We discuss the new VCSEL light source technology in Section 3. Anterior eye imaging at 1310nm is presented in Section 4 and imaging of various biological samples at different speeds from 60kHz – 1MHz axial scan rate is presented in Section 5. Concluding remarks are presented in Section 6, which summarizes the advantages of VCSEL based OCT imaging.

## 2. REVIEW OF OCT IMAGING TECHNOLOGIES

### 2.1 Time Domain and Spectral / Fourier Domain OCT – Today’s Dominant Commercial OCT Technologies

Early OCT systems used time domain detection<sup>1</sup>. Time domain OCT uses low coherence interferometry with a mechanically swept reference mirror to measure the echo delay of backscattered light. Time domain OCT can achieve a long imaging range, but is limited to imaging at very slow speeds of ~400-2000 axial scans per second. Fourier domain detection has a fundamental sensitivity advantage which enables orders of magnitude faster imaging speeds compared to time domain OCT<sup>8-11</sup>. Spectral / Fourier domain OCT (SD-OCT) uses a broadband light source, interferometer, spectrometer, and line scan camera. The maximum imaging range is determined by the spectrometer resolution. In commercial retinal systems, imaging range is typically limited to 2-3mm because of limitations in practical optical designs and available technologies. State of the art, commercial retinal OCT instruments sold today currently use SD-OCT technology and image at speeds of ~20,000 to ~50,000 axial scans per second.

SD-OCT systems exhibit a loss (roll-off) in sensitivity with increasing imaging depth due to spectrometer resolution limits, finite camera pixel width, aliasing at high spatial frequencies and interpixel cross-talk<sup>12, 13</sup>. Figure 1(A) shows the effect of OCT sensitivity roll-off for a SD-OCT system. When the retina is imaged at a shallow depth, the image has a high signal strength. If the retina is positioned further from the zero delay position in the imaging range, the signal strength decreases. At the full depth range, the image is unusable. The pronounced effect of sensitivity roll-off in commercial OCT instruments based on SD-OCT has led to the development of methods such as Enhanced Depth Imaging (EDI)<sup>14</sup>. EDI enables imaging the choroid by flipping the retinal image such that the choroid is imaged at a shallower depth with more sensitivity, but at a cost of reduced signal strength of inner retinal layers. The operator must choose to either image the inner retinal layers or the choroid with high signal strength, but part of the retina is always imaged with reduced sensitivity. This is a significant disadvantage of SD-OCT, which can be only somewhat mitigated by averaging multiple repeated or neighboring cross sectional scans in order to increase sensitivity.

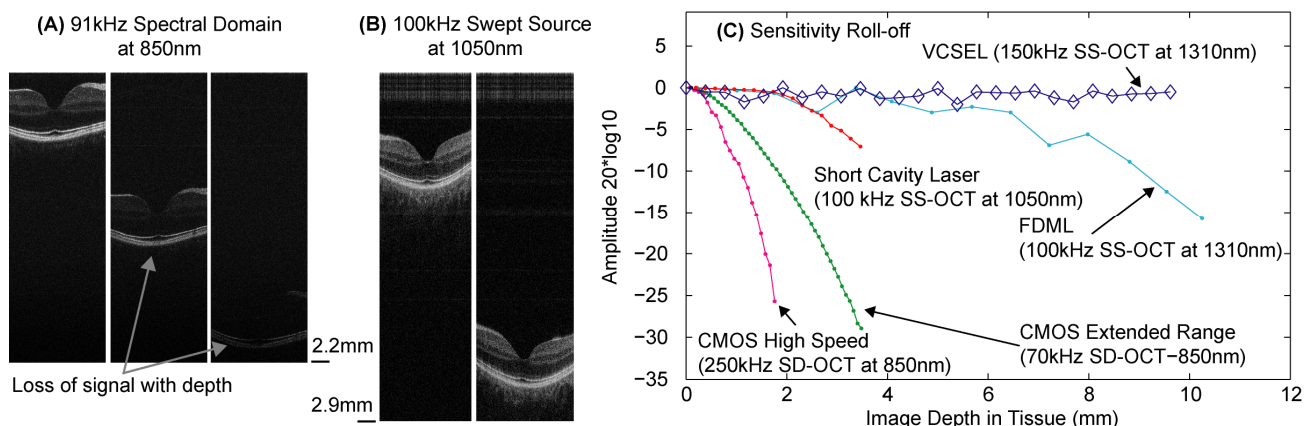


Figure 1. (A) Spectral domain OCT suffers from a loss of sensitivity with imaging depth. (B) Swept source OCT maintains the sensitivity through a deeper imaging depth. Images obtained with commercially available swept source. (C) VCSEL compared with competing options with respect to OCT sensitivity roll-off performance. The VCSEL significantly outperforms other OCT imaging technologies, enabling extended depth range OCT imaging.

## 2.2 Swept Source / Fourier Domain OCT – The Potential OCT Technology of the Future

Currently used in only a few medical instruments for ophthalmology and intravascular OCT imaging, swept source / Fourier domain OCT (SS-OCT) is an alternative OCT technology which offers several advantages compared with SD-OCT<sup>15-17</sup>. SS-OCT detects optical echo time delays by using an interferometer with a wavelength swept laser light source and detector with a high speed A/D converter. In SS-OCT, the swept laser linewidth determines the sensitivity roll-off with depth. Because the laser linewidth can be much narrower than a typical spectrometer resolution, SS-OCT can have significantly better sensitivity roll-off performance than SD-OCT, as shown in Fig. 1C<sup>18</sup>. SS-OCT also has the advantage that sample motion does not cause severe fringe washout effects, which results in loss of sensitivity with SD-OCT<sup>19</sup>. SS-OCT has the potential for superior sensitivity compared with SD-OCT because there are no spectrometer losses, detectors are more efficient than line scan cameras and dual balanced detection can be used. While the theoretical advantages of SS-OCT over SD-OCT have long been recognized by the OCT research community, progress has been limited by the lack of high performance, cost-effective swept laser source technologies.

## 2.3 Swept Laser Sources for SS-OCT

A variety of swept laser sources have been demonstrated for SS-OCT, including galvanometer-scanned mirrors and diffraction gratings, rotating polygons, and resonant galvo-scanned grating filters<sup>16, 20-23</sup>. Relatively long cavity lengths >10cm limited the maximum laser sweep repetition rates to a few tens of kHz in these bulk optics designs. Commercial short external cavity lasers (Axsun Technologies) have recently emerged and operate at 100kHz axial scan rate<sup>18</sup>. Short cavity lasers show improved sensitivity roll-off performance compared to SD-OCT as shown in Fig 1C. However, they operate with multiple longitudinal modes resulting in a broad effective laser linewidth, which degrades sensitivity roll-off performance and limits imaging range to ~5mm. Fourier Domain Mode Locked (FDML) lasers<sup>24</sup> have achieved record imaging speeds up to 1.4 MHz at 1050nm<sup>25</sup> and 5.2MHz at 1310nm<sup>26</sup>. FDML lasers operate best at 1310nm wavelengths with zero dispersion fiber, but have traditionally had poor performance at 1050nm with short coherence lengths of only ~1-2mm<sup>25, 27</sup>. It is therefore not clear that 1050nm FDML technology can effectively be used in the ophthalmology clinic.

## 3. VERTICAL CAVITY SURFACE EMISSION LASER (VCSEL) TECHNOLOGY

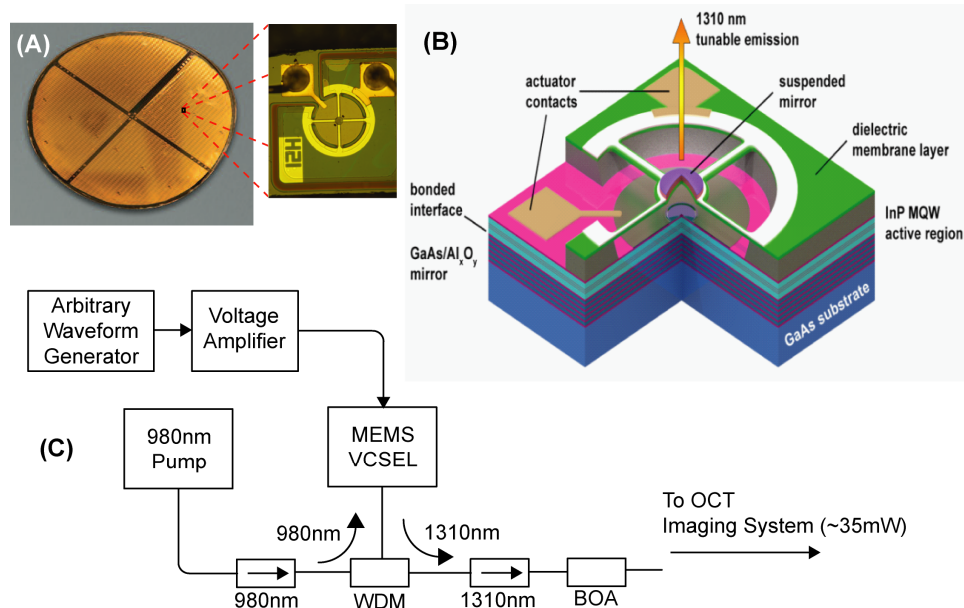


Figure 2. (A) Wafer of VCSELs with zoom showing wire bonded MEMS actuator (B) MEMS tunable VCSEL structure. (C) OCT light source schematic.

We have developed a new swept source laser technology based on a MEMS tunable Vertical Cavity Surface Emitting Laser (VCSEL)<sup>28</sup>. The integrated design of the VCSEL can be scaled to operate in different wavelength regimes ranging from 800nm to 1500nm and enables high volume production as shown in Fig. 2(A). A schematic diagram of a widely

tunable MEMS VCSEL is shown in Fig. 2(B). The VCSEL is optically pumped at 980nm and a low mass electrostatically tunable mirror enables high speed wavelength tuning centered at ~1310nm. As shown in Fig. 2(C), an arbitrary waveform generator and voltage amplifier drive the MEMS actuator. A semiconductor booster optical amplifier (BOA) increases the output power up to ~35mW while maintaining the intrinsic bandwidth of over 110nm, as shown in Fig. 3(A). The measured axial resolution is ~10um in tissue. The micron-scale cavity length of the VCSEL enables single mode operation without mode hopping. Consequently, the coherence length of the laser can be extremely long. Figure 3(B) shows the roll-off in OCT sensitivity as a function of imaging depth while dynamically tuning the 1310nm VCSEL at 150kHz over the full spectral bandwidth and after booster amplification (measured with 1.2GHz detectors and 5GSPS digital storage scope). There is only ~1.5dB measurable drop in sensitivity over a 50mm imaging range, indicating a coherence length much larger than 100mm in air. This is far superior to other technologies<sup>18, 27, 29, 30</sup> used in swept source OCT, as well as spectral / Fourier domain detection, as shown in Figure 1(C).

The dynamics of the device enable a relatively flat frequency response from ~50-500kHz. By adjusting the input drive waveform, the device can operate over a range of axial scan rates from ~50kHz - 1MHz. Figure 4 shows voltage drive waveforms, OCT MZI fringes, and the sweep trajectory for speeds of 100kHz-1.2MHz axial scans per second. Below the resonant frequency of the device, the sweep can be linearized to more efficiently utilize the A/D sampling rate and increase the imaging range of the instrument. Both the forwards and backwards sweeps can be used for imaging to achieve a high duty cycle and low peak fringe frequency compared to other swept laser technology which only provides good performance with one sweep direction. Optical clocking of the A/D converter has been shown to eliminate the need for software based sweep recalibration as well as to reduce data throughput and storage requirements. Other swept light sources have limited coherence length and optical clocking requires electrical frequency doubling of the interferometer signal to achieve adequate digitization rates at 2X the maximum fringe frequency to satisfy Nyquist sampling requirements<sup>31, 32</sup>. The long coherence length of the VCSEL enables a very high quality fringe at long interferometer path length differences, so that the optical interference signal can be used to clock the A/D directly, without requiring electronic frequency doubling.

The technical advantages of the VCSEL technology described above suggest that they are a near ideal light source for ophthalmic and other OCT applications. The wavelength scalability of the VCSEL should enable operation at 850 or 1050nm using similar wafer materials. The VCSEL provides a 20-40x increase in imaging speed compared to current clinical ophthalmic OCT technology, which will enable more comprehensive volumetric OCT data on retinal pathology as well as more accurate morphometry of the retina and anterior eye. Higher speed enables higher axial scan densities, thereby reducing the chance of missing small focal pathologies. In addition, higher speed reduces motion artifacts, thereby avoiding the need for hardware motion tracking systems and simplifying software-based, motion correction algorithms.

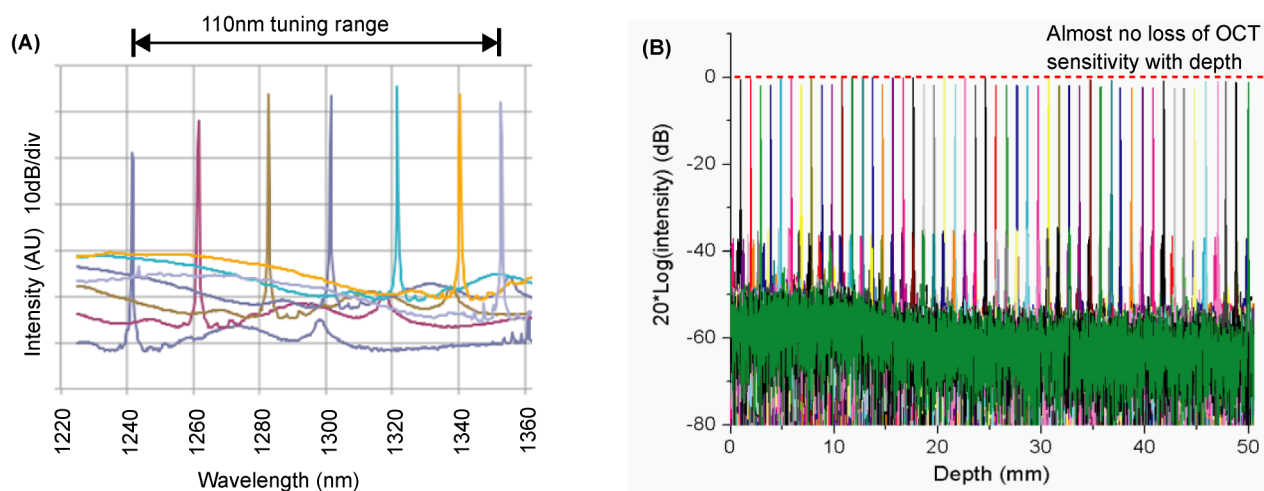


Figure 3. (A) Static operation of the device demonstrates 110nm of wavelength tuning in a 1310nm VCSEL. (B) 1310nm VCSEL achieves >50mm imaging range (>100mm coherence length) in air, demonstrated by negligible sensitivity reduction with depth.

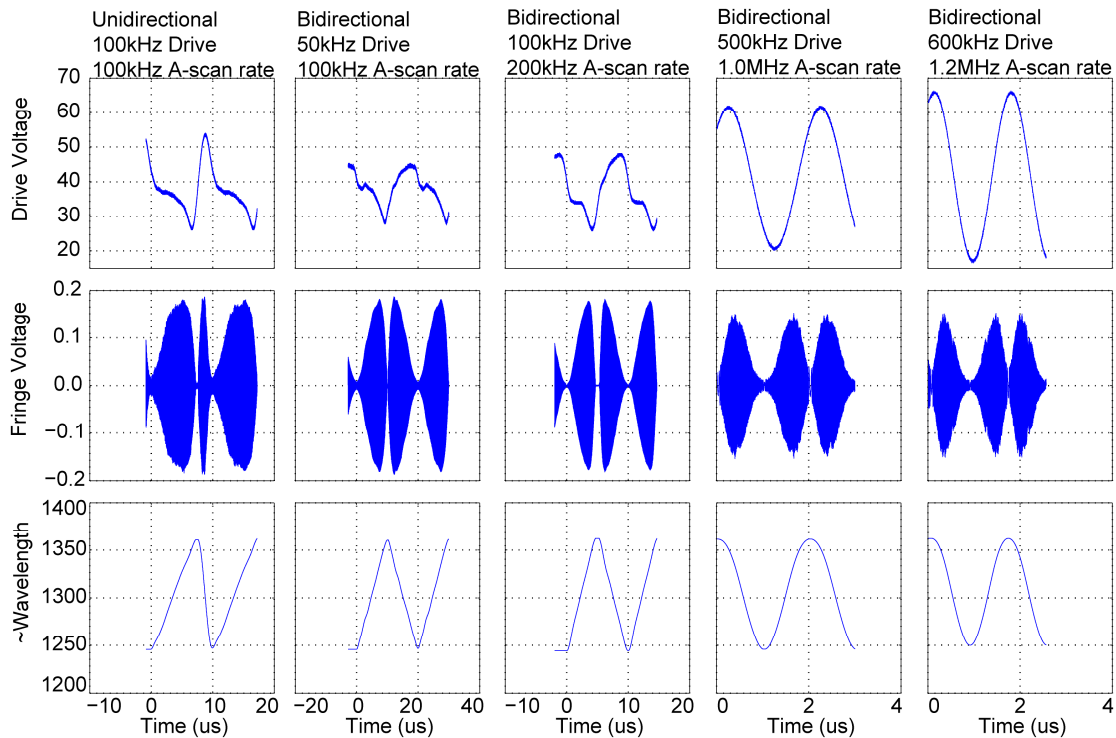


Figure 4. Single VCSEL driven by custom waveforms, over 115nm range, resulting in: (1) 100kHz drive/100kHz A-scan rate unidirectional linearized scan, (2) 50 kHz drive/100kHz A-scan rate bi-directional linearized scan, (3) 100 kHz drive/200kHz A-scan rate bi-directional linearized scan, (4) 500kHz drive/ 1 MHz A-scan rate bi-directional sinusoidal scan, and (5) 600kHz drive/ 1.2 MHz A-scan rate bi-directional sinusoidal scan.

#### 4. 1310NM ANTERIOR SEGMENT IMAGING

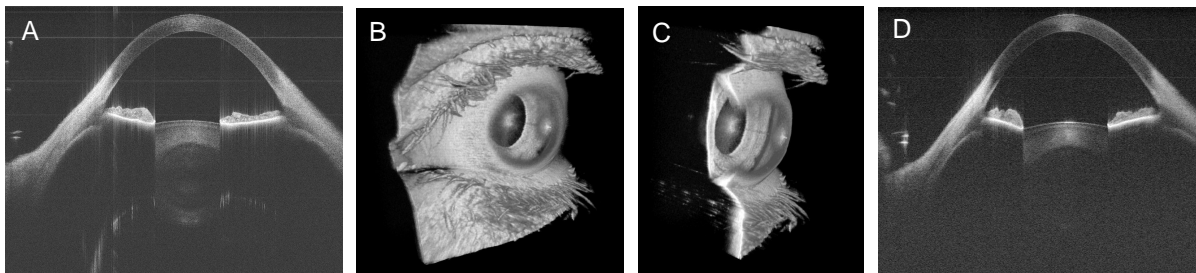


Figure 5. (A) OCT cross sectional image of the anterior eye consisting of 10,000 axial scans over 21mm obtained at 100,000 axial scans per second. (B) Rendering of a 400x400 axial scan volume of the anterior eye obtained at 100,000 axial scans per second. (C) Cutaway of the volume shows the iris in 3D and interior features. (D) OCT cross sectional image obtained by averaging 5 adjacent B-scans from the 400x400 axial scan volume.

OCT systems dedicated to imaging the anterior eye use longer 1310nm wavelengths for reduced scattering and deeper penetration into tissue. Figure 5 shows preliminary anterior segment imaging results obtained with a 1310nm VCSEL. Imaging of the anterior eye was performed in normal human subjects using a telecentric scanning interface with a 0.024NA beam. Figure 5(A) shows an OCT cross sectional image of the anterior eye obtained at 100,000 axial scans per second. The long coherence length of the VCSEL laser enables a long imaging range extending from the cornea to the posterior lens surface. Linearization of the frequency sweep combined with the ability to use both the forwards and backwards sweeps gives a high duty cycle and efficient utilization of A/D bandwidth. The A/D converter is optically clocked using the VCSEL output and a MZI interferometer, avoiding the need for sweep recalibration. The peak A/D sampling rate for the image in Fig. 5(A) is only ~380MSPS. Consequently, commonly available and relatively low cost 400-500MSPS A/D converters with 12-14bits of resolution can be used to obtain long OCT imaging range with the

VCSEL source. The reduced data transfer requirements for optically clocked data<sup>18</sup> and ability to achieve a long imaging range using moderate A/D sampling rates are attractive for commercialization and integration into OCT imaging products. Figure 5(B) and 5(C) show a 3D OCT volume of the anterior eye consisting of 400x400 axial scans over a 21mm x 21mm area acquired in 1.9 seconds (including galvo flyback) at 100,000 axial scans per second imaging rate. Minimal motion artifacts are visible and comprehensive structural information from the entire corneal surface, iris and crystalline lens is available, which promises to aid in diagnosing disease, as well as improving refractive surgery. Figure 5(D) shows an OCT cross sectional image obtained by averaging 5 adjacent B-scans in the 3D volume. Signal to noise is improved and speckle is reduced to yield a high contrast image, although lateral and axial resolution are slightly degraded by merging of neighboring morphological features.

### 5. 1310NM VARIABLE RATE IMAGING

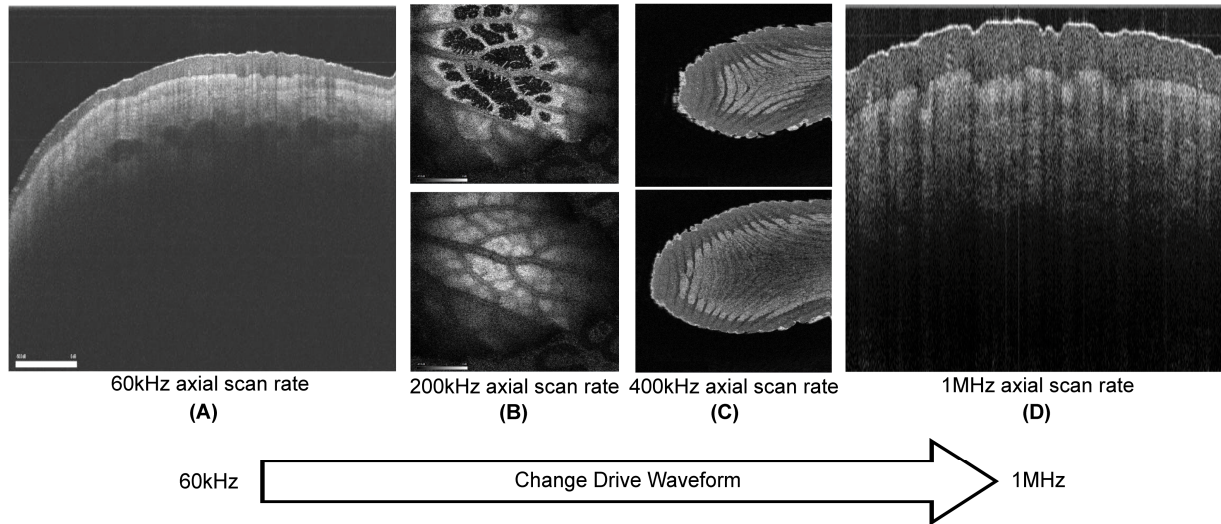


Figure 6. Variable speed OCT imaging (A) OCT cross sectional image of human finger showing blood vessels and long imaging range acquired at 60kHz. (B) OCT en face images of a plant leaf consisting of 340x300 axial scans over 6mmx6mm acquired at 200,000 axial scans per second. (C) OCT en face images of a finger pad consisting of 512x512 axial scans over 6.3mmx6.3mm acquired at 400,000 axial scans per second. (D) OCT cross sectional image of a finger pad consisting of 4096 axial scans over 5mm acquired at 1MHz axial scan rate.

Figure 6 shows images obtained at speeds of 60kHz – 1MHz with a 1310nm VCSEL. An OCT cross sectional image of a human finger is shown in Fig. 6(A). OCT en face images of a plant leaf extracted from a 3D volume obtained at 200,000 axial scans per second are shown in Fig. 3(B). Figure 3(C) shows an en face OCT image of a human finger pad obtained at 400,000 axial scans per second using a bidirectional sweep. The extremely high axial scan rates of VCSEL technology will enable rapid acquisition of large 3D OCT data sets which are required for en face imaging. Figure 3(D) shows a cross sectional OCT image of the finger obtained at 1,000,000 (1MHz) axial scans per second. Fingerprint ridges, sweat glands, and dermal layers can be seen with high detail and contrast, indicating the capability of OCT imaging with this new light source at ultrahigh speeds approximately an order of magnitude faster than existing commercial OCT technologies.

### 6. CONCLUSIONS

New MEMS tunable VCSEL light source technology achieves record long coherence lengths and can sweep over a wide range of speeds. Enabled by a short micron scale length laser cavity, the VCSEL is unique in its ability to achieve high speed 100's of kHz scan rates with negligible sensitivity drop over centimeter scale imaging ranges. VCSEL based OCT imaging achieves higher speed imaging than commercial time domain OCT anterior imaging systems, enabling acquisition of densely sampled 3D volumes of the cornea, iris, and crystalline lens. Results presented in this paper are preliminary. We show comprehensive characterization of a 2<sup>nd</sup> generation 1310nm VCSEL device and demonstrate the ability to achieve a wide range of sweep speeds and trajectories by using custom drive waveforms. Bidirectional scanning and high duty cycle allows for long imaging range with moderate A/D rates of 400MSPS for anterior eye

imaging. The 1310nm VCSEL was the first prototype developed and is currently in a second generation design. However, while 1310nm wavelengths work well for imaging the anterior eye, water absorption in the vitreous precludes use of 1310nm wavelengths for imaging of the retina. We have recently demonstrated a 1050nm optically pumped VCSEL with 100nm tuning range for retinal and anterior eye imaging applications, as shown in Fig. 7.

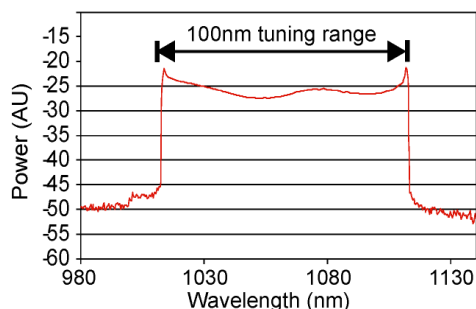


Figure 7. Spectral tuning range for first generation prototype optically pumped 1050nm VCSEL.

These results suggest that VCSEL source technology will have a unique and important impact on OCT imaging for a wide range of applications. The high sweep speed and unequalled long coherence length of the VCSEL promise to improve the data density, quality, and usable imaging range of OCT images. Because of the wafer based large scale manufacturing techniques, it is envisioned that the cost of the VCSEL could be made quite low, possibly increasing accessibility to OCT instrumentation for use in developing countries, screening in optometry, and possibly even screening at the primary care physician point of care.

**ACKNOWLEDGEMENTS:** This research was supported in part by NIH 2R44CA10167-05, R01-EY011289-25, R01-EY01356-06, R01-EY013178-11, R01-CA075289-15, AFOSR FA9550-10-1-0063 and FA9550-10-1-0551, and at Praevium Research by Thorlabs matching funds.

## REFERENCES

- [1] D. Huang, E. A. Swanson, C. P. Lin, J. S. Schuman, W. G. Stinson, W. Chang, M. R. Hee, T. Flotte, K. Gregory, C. A. Puliafito, and J. G. Fujimoto, "Optical Coherence Tomography," *Science*, 254(5035), 1178-1181 (1991).
- [2] C. A. Puliafito, M. R. Hee, C. P. Lin, E. Reichel, J. S. Schuman, J. S. Duker, J. A. Izatt, E. A. Swanson, and J. G. Fujimoto, "Imaging of macular diseases with optical coherence tomography," *Ophthalmology*, 102(2), 217-229 (1995).
- [3] M. R. Hee, J. A. Izatt, E. A. Swanson, D. Huang, J. S. Schuman, C. P. Lin, C. A. Puliafito, and J. G. Fujimoto, "Optical coherence tomography of the human retina," *Archives of Ophthalmology*, 113(3), 325-332 (1995).
- [4] W. Drexler, U. Morgner, R. K. Ghanta, F. X. Kärtner, J. S. Schuman, and J. G. Fujimoto, "Ultrahigh-resolution ophthalmic optical coherence tomography," *Nature Medicine*, 7(4), 502-507 (2001).
- [5] J. S. Schuman, C. A. Puliafito, and J. G. Fujimoto, [Optical coherence tomography of ocular diseases, 2nd edition] Slack Inc., Thorofare, NJ(2004).
- [6] E. A. Swanson, and D. Huang, "Ophthalmic OCT Reaches \$1 Billion Per Year," *Retinal Physician*, 8(4)(MAY 2011), 45,58-59,62 (2011).
- [7] D. Huang, J. S. Duker, J. G. Fujimoto, B. Lumbroso, J. S. Schuman, and R. N. Weinreb, [Imaging the Eye from Front to Back with RTVue Fourier-Domain Optical Coherence Tomography] Slack Publishing, (2010).
- [8] A. F. Fercher, C. K. Hitzenberger, G. Kamp, and S. Y. Elzaiat, "Measurement of Intraocular Distances by Backscattering Spectral Interferometry," *Optics Communications*, 117(1-2), 43-48 (1995).
- [9] R. Leitgeb, C. K. Hitzenberger, and A. F. Fercher, "Performance of Fourier domain vs. time domain optical coherence tomography," *Optics Express*, 11(8), 889-894 (2003).
- [10] J. F. de Boer, B. Cense, B. H. Park, M. C. Pierce, G. J. Tearney, and B. E. Bouma, "Improved signal-to-noise ratio in spectral-domain compared with time-domain optical coherence tomography," *Optics Letters*, 28(21), 2067-2069 (2003).

- [11] M. A. Choma, M. V. Sarunic, C. H. Yang, and J. A. Izatt, "Sensitivity advantage of swept source and Fourier domain optical coherence tomography," *Optics Express*, 11(18), 2183-2189 (2003).
- [12] Z. Hu, Y. Pan, and A. M. Rollins, "Analytical model of spectrometer-based two-beam spectral interferometry," *Appl. Opt.*, 46(35), 8499-8505 (2007).
- [13] T. Bajraszewski, M. Wojtkowski, M. Szkulmowski, A. Szkulmowska, R. Huber, and A. Kowalczyk, "Improved spectral optical coherence tomography using optical frequency comb," *Optics Express*, 16(6), 4163-4176 (2008).
- [14] R. F. Spaide, H. Koizumi, and M. C. Pozzoni, "Enhanced depth imaging spectral-domain optical coherence tomography," *American Journal of Ophthalmology*, 146(4), 496-500 (2008).
- [15] B. Golubovic, B. E. Bouma, G. J. Tearney, and J. G. Fujimoto, "Optical frequency-domain reflectometry using rapid wavelength tuning of a Cr<sup>4+</sup>:forsterite laser," *Optics Letters*, 22(22), 1704-1706 (1997).
- [16] S. R. Chinn, E. A. Swanson, and J. G. Fujimoto, "Optical coherence tomography using a frequency-tunable optical source," *Optics Letters*, 22(5), 340-342 (1997).
- [17] S. H. Yun, G. J. Tearney, B. E. Bouma, B. H. Park, and J. F. de Boer, "High-speed spectral-domain optical coherence tomography at 1.3  $\mu$ m wavelength," *Optics Express*, 11(26), 3598-3604 (2003).
- [18] B. Potsaid, B. Baumann, D. Huang, S. Barry, A. E. Cable, J. S. Schuman, J. S. Duker, and J. G. Fujimoto, "Ultrahigh speed 1050nm swept source / Fourier domain OCT retinal and anterior segment imaging at 100,000 to 400,000 axial scans per second," *Optics Express*, 18(19), 20029-20048 (2010).
- [19] S. H. Yun, G. J. Tearney, J. F. de Boer, and B. E. Bouma, "Motion artifacts in optical coherence tomography with frequency-domain ranging," *Optics Express*, 12(13), 2977-2998 (2004).
- [20] E. C. W. Lee, J. F. de Boer, M. Mujat, H. Lim, and S. H. Yun, "In vivo optical frequency domain imaging of human retina and choroid," *Optics Express*, 14(10), 4403-4411 (2006).
- [21] H. Lim, J. F. de Boer, B. H. Park, E. C. W. Lee, R. Yelin, and S. H. Yun, "Optical frequency domain imaging with a rapidly swept laser in the 815-870 nm range," *Optics Express*, 14(13), 5937-5944 (2006).
- [22] V. J. Srinivasan, R. Huber, I. Gorczynska, J. G. Fujimoto, J. Y. Jiang, P. Reisen, and A. E. Cable, "High-speed, high-resolution optical coherence tomography retinal imaging with a frequency-swept laser at 850 nm," *Optics Letters*, 32(4), 361-363 (2007).
- [23] D. M. de Bruin, D. L. Burnes, J. Loewenstein, Y. Chen, S. Chang, T. C. Chen, D. D. Esmaili, and J. F. de Boer, "In vivo three-dimensional imaging of neovascular age-related macular degeneration using optical frequency domain imaging at 1050 nm," *Invest Ophthalmol Vis Sci*, 49(10), 4545-52 (2008).
- [24] R. Huber, M. Wojtkowski, and J. G. Fujimoto, "Fourier Domain Mode Locking (FDML): A new laser operating regime and applications for optical coherence tomography," *Optics Express*, 14(8), 3225-3237 (2006).
- [25] T. Klein, W. Wieser, C. M. Eigenwillig, B. R. Biedermann, and R. Huber, "Megahertz OCT for ultrawide-field retinal imaging with a 1050nm Fourier domain mode-locked laser," *Optics Express*, 19(4), 3044-3062 (2011).
- [26] W. Wieser, B. R. Biedermann, T. Klein, C. M. Eigenwillig, and R. Huber, "Multi-Megahertz OCT: High quality 3D imaging at 20 million A-scans and 4.5 GVoxels per second," *Optics Express*, 18(14), 14685-14704 (2010).
- [27] D. C. Adler, W. Wieser, F. Trepanier, J. M. Schmitt, and R. A. Huber, "Extended coherence length Fourier domain mode locked lasers at 1310 nm," *Optics Express*, 19(21), 20930-20939 (2011).
- [28] V. Jayaraman, J. Jiang, H. Li, P. J. S. Heim, G. D. Cole, B. Potsaid, J. G. Fujimoto, and A. Cable, "OCT imaging up to 760 kHz axial scan rate using single-mode 1310nm MEMS-tunable VCSELs with >100nm tuning range." *Lasers and Electro-Optics (CLEO) Conference*, 1-2 (2011).
- [29] B. Potsaid, I. Gorczynska, V. J. Srinivasan, Y. L. Chen, J. Jiang, A. Cable, and J. G. Fujimoto, "Ultrahigh speed Spectral/Fourier domain OCT ophthalmic imaging at 70,000 to 312,500 axial scans per second," *Optics Express*, 16(19), 15149-15169 (2008).
- [30] S. Marschall, T. Klein, W. Wieser, B. Biedermann, K. Hsu, B. Sumpf, K. H. Hasler, G. Erbert, O. B. Jensen, C. Pedersen, R. Huber, and P. E. Andersen, "FDML swept source at 1060 nm using a tapered amplifier," *Optical Coherence Tomography and Coherence Domain Optical Methods in Biomedicine Xiv*, 7554, (2010).
- [31] D. C. Adler, Y. Chen, R. Huber, J. Schmitt, J. Connolly, and J. G. Fujimoto, "Three-dimensional endomicroscopy using optical coherence tomography," *Nature Photonics*, 1(12), 709-716 (2007).
- [32] J. F. Xi, L. Huo, J. S. Li, and X. D. Li, "Generic real-time uniform K-space sampling method for high-speed swept-Source optical coherence tomography," *Optics Express*, 18(9), 9511-9517 (2010).